Ibn Al-Haitham Journal for Pure and Applied Sciences
Journal homepage: jih.uobaghdad.edu.iq
PISSN: 1609-4042, EISSN: 2521-3407
IHJPAS. 2025, 38(3)

Study and Investigation of the Charge Transfer Rate Production in N3-Senstized Dye Contact with ZnS Semiconductor System

Zainab A. Hamid[1] and Mohsin A. Hassooni[2*]
[1,2] Department of Physics, College of Education for Pure Science (Ibn Al-Haitham), University of Baghdad, Baghdad-Iraq.
*Corresponding Author.

Received: 18 January 2025 Accepted: 3 March 2025 Published: 20 July 2025
doi.org/10.30526/38.3.4114

Abstract

In this work, the rate of charge transfer (CT) reaction at the N3-ZnS interface was calculated using a quantitative computational model to evaluate the efficiency of N3-ZnS heterojunction dye-sensitized solar cell devices using different types of solvents. This work discussed the influence of the effective driving energy force on the charge transport rate and performance of N3-ZnS devices with various solvents based on a donor-acceptor model. A solar cell model was used to study the optical efficiency when changing some of its parameters, such as the type of material and the thickness of the film, as they are important factors influencing the quality of the solar cell. It was found that the transition energy varies with different solvent types depending on the dielectric constant, refractive index of the solvent, and the semiconductor, the electron transfer rate increased when the effective driving force value decreased to Δ^0 =0.22 (eV) at the same temperature and charge carrier concentration, where the maximum value of the electron transfer rate for chloroform solvent was (1.0622E-06).

Keywords: Effective driving force, N3 dye, ZnS Semiconductor, Charge transfer.

1. Introduction

Increasing energy consumption, depletion of fossil resources, and greenhouse gas emissions are major environmental challenges that have prompted extensive efforts to develop clean and renewable energy sources (1). Among the promising solutions, many experimental and theoretical approaches have been harnessed to understand and optimize dye-sensitized solar cells (DSSCs), to achieve high cell performance while using environmentally friendly materials and reducing manufacturing costs, making them an outstanding choice for photovoltaic (PV) conversion (2). Among the several types of photovoltaic devices created in recent decades, dye-sensitized solar cells (DSSCs) have sparked increased interest, with noteworthy advances in performance. This has been made feasible by extensive research into each of the components of these cells, which aim to optimize the sensitizer, electrolytic mixture, and production process (3).

Consequently, a great deal of research has been conducted to comprehend the dynamics of charge carriers (transport characteristics) at the dye-semiconductor interface of DSSCs (4) .To promote the CT from the sensitive dye to the semiconductor's conduction band, the dye in the DSSC solar cell absorbs light for excitation. It then replenishes the oxidized dye molecules by donating electrons from the redox pair of the system, and convection completes the charge transfer (5). One of the basic models used to study electron transport is the donor-acceptor model, which is characterized by the fact that no chemical bonds are formed or broken within the system. Moreover, the contact region between molecules and semiconductor systems has received increasing attention in many technical applications, and its CT occurs across this interface (6).

Hadi et al conducted a study on the CT reaction process in heterostructure systems, based on orientation energy analysis and compatibility of energy levels between materials used in electronic devices. It was found that the transfer of electrons between different states requires convergence of the energy levels of both materials (7). The CT in these devices depends on the transitions in energy states between the donor and acceptor at the contact interface in the heterostructures. Recently, research has focused on developing new device designs, along with optimizing sensors and reductive mediators, to enhance the performance efficiency of DSSCs (8).The chromophore (cis-bis (isothiocyanato) bis (2,2′ -bipyridyl-4,4′-dicarboxylato ruthenium (II), generally known as N3 dye, is an effective and popular dye used in photocatalytic, photoelectrochemical, and DSSC devices (9). The electronic shift from the highest occupied molecular orbital (HOMO) to the lowest unoccupied molecular orbital (LUMO) is the main cause of N3 dye's exceptional ability to absorb sunlight. N3, once elevated to an electronically excited state, can transport an electron to the CB of a semiconductor. Because charge transfer reactions are spatially dependent, the N3 dye's LUMO electron density is optimally situated close to the semiconductor surface to promote advantageous charge transfer from the dye to the semiconductor (10,11). Its structure is shown in **Figure (1**)(12). Zinc sulfide (ZnS), a semiconductor with important electrical and optical characteristics, shows promise as a material for solar cell applications. Its broad bandgap, which normally falls between 3.47 and 3.9 eV, enables efficient light conversion and absorption in solar systems (13). It is well known that quantum confinement occurs when scale constraints influence electronic wavefunctions. The long-term application of quantum-confined ZnS is predicted to dominate material production in numerous key fields within the next decade, including semiconductors, optoelectronics, and solar cells. Several wet-chemical processes have already been used to successfully manufacture ZnS. Although ZnS exhibits a lot of promise for solar cell applications, there are still issues with optimizing its production and incorporating it into current technology. Further investigations are required to properly utilize its potential in photovoltaic (14). The main objective of this work was to study and calculate the CT rate in N3-ZnS heterojunction device and discuss the force coupling, transition energy, driving energy and voltage at a specific temperature.

2. Materials and Methods

The computation of the electronic transport coefficient for the N3-ZnS system can be approached by representing the system within the Hilbert space framework. The time-dependent nature of electronic transport between the N3 donor and ZnS acceptor allows it to be analyzed using perturbation theory. Within this framework, the complete wave functions

for the states of the N3 donor and ZnS acceptor are expressed in terms of the Hilbert space representation (15).

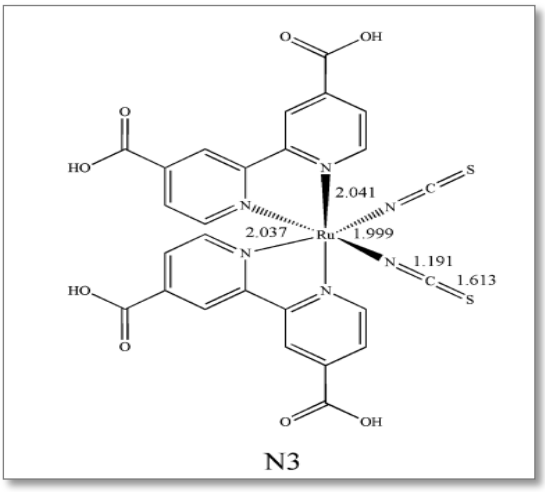

Figure 1. Structure of N3 dye.

$$|\psi_n(r,t)\rangle = (|\phi_{N3}\rangle + |\phi_{ZnS}\rangle)e^{\frac{-i}{\hbar}E_n t} \quad (1)$$

This equation represents the system's quantum state which combines the donor and acceptor in the form of a total wave function. (16)Under the non-adiabatic approximation, the electrons satisfy the Schrodinger equation, which describes the state of the electrons interacting in the donor-acceptor system, reads:

$$\widehat{E}_S(|\phi_{N3}\rangle + |\phi_{ZnS}\rangle)e^{\frac{-i}{\hbar}E_n t} = i\hbar\frac{\partial}{\partial t}(|\phi_{N3}\rangle + |\phi_{ZnS}\rangle)e^{\frac{-i}{\hbar}E_n t} \quad (2)$$

Describes the evolution of the quantum state of a system over time using the Hamiltonian operator.

$$(\widehat{\mathcal{H}}_{N3} + \widehat{\mathcal{H}}_{ZnS})\left(\sum_i^\infty D_i\,|\phi_{N3}(r)\rangle + \sum_j^\infty A_j\,|\phi_{ZnS}(r)\rangle\right)e^{\frac{-i}{\hbar}E_n t}) = i\hbar\sum_{i,j}^\infty\left[D_i\frac{\partial|\phi_{N3}(r)\rangle}{\partial t} + A_j\frac{\partial|\phi_{ZnS}(r)\rangle}{\partial t}\right]e^{-i\frac{E_n t}{\hbar}} \quad (3)$$

This equation shows how the interaction between donor and acceptor affects the overall wave function.

$$\left\langle\psi_n(r,t)\left|\widehat{\mathcal{H}}_{\frac{N3}{ZnS}}\right|\psi_n(r,t)\right\rangle =$$

$$i\hbar\sum_{i,j}^\infty e^{-i\frac{E_n t}{\hbar}}\left[\frac{\partial D_i}{\partial t}\,D_i{}^*|\phi_{N3}(r)\rangle\langle\phi_{N3}(r)| + \frac{\partial A_j}{\partial t}\,A_j{}^*|\phi_{ZnS}(r)\rangle\langle\phi_{ZnS}(r)|\right]e^{\frac{+i}{\hbar}E_n t} \quad (4)$$

This represents the interference coefficient between electrons in the system, based on the energy difference (17).

The quantity of the square magnitude of C_{DA} indicate the probability of density (18).

$$\rho_{DA} = |C_{DA}|^2 \quad (5)$$

Thus, it becomes

$$\rho_{DA} = \frac{\left|\langle\widehat{\mathcal{H}}_{\frac{N3}{ZnS}}\rangle\right|^2}{\hbar^2}\left|\frac{(e^{-\frac{i}{\hbar}(E_{N3}-E_{ZnS})t}-1)}{\frac{(E_{N3}-E_{ZnS})}{\hbar}}\right|^2 \quad (6)$$

Consequently, the absolute value in Eq. (6) can be simplified to:

$$\left|\frac{(e^{-\frac{i}{\hbar}(E_{N3}-E_{ZnS})t}-1)}{(E_{N3}-E_{ZnS})}\right|^2 = \frac{4\hbar}{(E_{N3}-E_{ZnS})^2}sin^2(\frac{(E_{N3}-E_{ZnS})t}{2\hbar}) \quad (7)$$

Shows the effect of time on the probability of electronic transition (19).

$$\lim_{t\to\infty}\left(\frac{sin^2xt}{x^2t}\right)=\pi t\delta(x) \quad (8)$$

Equation (8) relies on mathematical techniques to describe the effect of time on the probability of an electronic transition between two quantum states in the system (N3 and ZnS). This formula shows that charge transfer occurs when the energy difference between donor and acceptor is appropriate and coincides with time changes.

The probability transfers are reduced to the transition rate by (20).

$$\Gamma=\frac{2\pi}{\hbar}\left|\langle\widehat{\mathcal{H}}_{\frac{N3}{ZnS}}\rangle\right|^2\delta(E_{N3}-E_{ZnS}) \quad (9)$$

The base set wave function of the dN3 donor and ZnS acceptor in the system $|\psi_n(r,t)\rangle$ must be orthonormal (21).

$$|\phi_{N3}(r)\rangle\langle\phi_{N3}(r)|=|\phi_{ZnS}(r)\rangle\langle\phi_{ZnS}(r)|=1 \quad (10)$$

The expectation values of the density of the state $\langle\hat{\rho}_{(E)}\rangle$ for electrons in the system with basic donor and acceptor states are (22, 23).

$$\langle\hat{\rho}_{(E)}\rangle=\sum_n^\infty\langle\psi_n(r,t)|\phi_{ZnS}(r)\rangle\left\langle\phi_{ZnS}(r)\middle|\hat{\rho}_{(E)}\middle|\phi_{N3}(r)\right\rangle\langle\phi_{N3}(r)|\psi_n(r,t)\rangle \quad (11)$$

$$\langle\hat{\rho}_{(E)}\rangle=N_{\frac{N3}{ZnS}}e^{\frac{-\Delta E_{\frac{N3}{ZnS}}}{k_BT}} \quad (12)$$

Based on the classical Marcus theory, the $\Delta E_{\frac{N3}{ZnS}}(eV)$ of the system is given by (24) .

$$\Delta E_{\frac{N3}{ZnS}}=\frac{(\Lambda_{N3/ZnS}+\Delta^0)^2}{4\Lambda_{N3/ZnS}} \quad (13)$$

where $\Lambda_{\mathrm{N3/ZnS}}$ is the transition energy of $\mathrm{N3/ZnS}$ systems and Δ^0 is the driving force of electrons.by substituting Eq. (13) in Eq. (12) to obtain

$$\langle\hat{\rho}_{(E)}\rangle=N_{\frac{N3}{ZnS}}\ e^{-\frac{(\Lambda_{N3/ZnS}+\Delta^0)^2}{4\Lambda_{N3/ZnS}}} \quad (14)$$

$$\Pi_{et}=\frac{2\pi}{\hbar}\frac{\left|\langle\widehat{\mathcal{H}}_{\frac{N3}{ZnS}}\rangle\right|^2}{\alpha}\sqrt{\frac{1}{4\pi\Lambda_{\frac{N3}{ZnS}}k_BT}}e^{-\frac{\left(\Lambda_{\frac{N3}{ZnS}}+\Delta^0\right)^2}{4\Lambda_{\frac{N3}{ZnS}}k_BT}}\frac{I_e}{\sqrt[3]{\frac{6d_a^2}{\pi}}}N_s(E) \quad (15)$$

The transition energy of the solvent circumfluent the system at the new equilibrium of the system is (25).

$$\Lambda_{N3/ZnS}(eV)=\frac{e^2}{8\pi\varepsilon_0}\frac{1}{D_{dye}}\left(\frac{1}{{n_{so}}^2}-\frac{1}{\epsilon_{so}}\right)-\frac{e^2}{16R\pi\varepsilon_0}\left(\frac{n_{Se}^2-{n_{so}}^2}{n_{Se}^2+{n_{so}}^2}\frac{1}{{n_{so}}^2}-\frac{\epsilon_{Se}^2-{\epsilon_{so}}^2}{\epsilon_{Se}^2+\epsilon{\epsilon_{so}}^2}\frac{1}{{\epsilon_{so}}^2}\right) \quad (16)$$

where e is the electron charge, ε_0 is permittivity D and R are the radius of the dye and the distance between the dye and the semiconductor, n_{se} and ϵ_{se} are the refractive index and dielectric constant of the semiconductor, n_{so} and ϵ_{so} the optical and statistical dielectric constants of solvents. The radius of the dye molecule is (26) .

$$r(m)=\sqrt[3]{\frac{3}{4\pi}\frac{M}{N_A\rho}} \quad (17)$$

Where M is the molecular weight, N_A is the Avogadro number, and ρ is the mass density.

3. Results

To understand the charge transfer behavior at the dye-semiconductor interface, a quantitative computational approach based on the quantum picture and assumed continuum state for all materials were used, using MATLAB software, to calculate the charge transfer rates in the N3-ZnS system with different solvents (Chloroform, (1,2-Dichloroethane), (1-

Methyl-2-pyrrolidinon) 1-Butanol and 1-Propano). The charge transfer rates from the excited dye to the semiconductor were calculated by determining the important parameters that play a key role in the charge transfer process. The transition energy was calculated using the Eq. (16), Based on the radii of N3 and ZnS as well as the refractive index and dielectric constant of ZnS and the solvents used, the values were determined using the equation (17) taking into account the molecular weight and mass density of the N3 dye according to **Table (1)** and the molecular weight and density for ZnS semiconductor **Table (2)**, it was found that the radius of the N3 dye was $R_{N3} = 5.9\ A^0$ while the radius of ZnS was $R_{Zns} = 2.115$ (Å). where the transition energy played the main and effective role in limiting the charge transfer process.

Table 1. Characteristics of N3 dye molecules (9,27-28)

The N3 Molecule dye	
Name of Dye	Cis-bis(isothiocyanato)bis(2,2′-bipyridyl-4,4′-dicarboxylato)ruthenium(II)
Chemical formula	($C_{26}H_{16}N_6O_8RuS_2$)
Molar Mass	705.64 g/mol
Density	1.36 g/cm^3
Melting point	$> 300C^o$
HOMO	-5.39 eV
LUMO	-2.79 eV
Calculated radius	5.9 A^o

Table 2. General properties of ZnS semiconductor (29, 30).

Properties	**ZnS**
Crystal Structure	Cubic
Molecular Weight	97.46 g/mol
Lattice Constant	5.4093 Å
Refractive Index	2.356
Band Gap	3.54 eV
Thermal Conductivity	25.1 W/mK
Density	4.079 g/cm^3
Melting Point	1850°C
Dielectric Constant	8.9
Radii	2.1158115 (Å)

From Eq.(16), the transition energy $\Lambda_{N3/ZnS}(eV)$ values of the N3-ZnS system were calculated by entering the refractive index and dielectric constant values of the ZnS semiconductor from **Table (2)** and the dielectric constant and refractive index values of the solvents used in the system, the transition energy values were obtained in **Table (3**), where the lowest value was for solvent Chloroform and the maximum value appeared when solvent 1-Propanol was used.

Table 3. Results of the reorientation energy $\Lambda(n, \epsilon)$ for charge transfer at N3-ZnS

Solvent	$\boldsymbol{\epsilon_{so}}$**(31)**	$\boldsymbol{n_{so}}$**(31)**	$\boldsymbol{\Lambda(n, \epsilon)}$
Chloroform	4.81	1.446	0.24323
1,2-Dichloroethane	9.08	1.424	0.36421
1-Methyl-2-pyrrolidinone	32.00	1.470	0.43471
1-Butanol	17.80	1.399	0.44411
1-Propanol	20.1	1.384	0.46131

Using equation (15), the CT rate was calculated by entering the values of the effective driving energy for N3/ZnS system $\Delta^0 = 0.22$ (eV), $\Delta^0 = 0.27$ (eV) and $\Delta^0 = 0.32$ (eV), and the concentration of charge carriers $N_e = 1.4 \times 10^{20} m^{-3}$ (32) at a temperature of 300k , taken the transition energy $\Lambda_{N3/ZnS}(eV)$ for N3/ ZnS with solvents coupling strength $\left|\langle \mathcal{H}_{\frac{ZnS}{N3}}(E)\rangle\right|^2 = (1\,x\,10^{-3})\ to\ (4x\,10^{-3})\ |eV|^2$ (33), effective length $l_e = 3A^0$ (34), atomic density $d_{ZnS} = 2.52039\,x10^{25}\,\frac{1}{m^3}$ and electronic concentration $\alpha = 1 \times 10^{10}\,\frac{1}{m}$ with MATLAP program, the results are listed in **Tables** from **(4), (5),** and **(6)**, and for N3/ZnS devices at effective driving energy $\Delta^0 = 0.22$ (eV) , $\Delta^0 = 0.27$ (eV) and $\Delta^0 = 0.32$ (eV) respectively.

Table 4. Results of CT rate production for N3- ZnS device system at $\Delta^0 = 0.22\ (eV)$ with $T = 300\ K$.

solvent	$\Lambda_{N3/ZnS}(eV)$	**Rate of Electronic Transfer cm^2/ Sec** $\langle \widehat{\mathcal{H}}_{\frac{N3}{ZnS}} \rangle$ **(eV)^2**						
		1×10^{-3}	**1.5×10^{-3}**	**2×10^{-3}**	**2.5×10^{-3}**	**3×10^{-3}**	**3.5×10^{-3}**	**4×10^{-3}**
Chloroform	0.24323	2.6554E-07	3.9831E-07	5.3108E-07	6.6385E-07	7.9662E-07	9.2940E-07	1.0622E-06
1,2-Dichloroethane	0.36421	1.2769E-07	1.9154E-07	2.5538E-07	3.1923E-07	3.8307E-07	4.4692E-07	5.1076E-07
1-Methyl-2-pyrrolidinone	0.43471	7.2837E-08	1.0926E-07	1.4567E-07	1.8209E-07	2.1851E-07	2.5493E-07	2.9135E-07
1-Butanol	0.44411	6.7320E-08	1.0098E-07	1.3464E-07	1.6830E-07	2.0196E-07	2.3562E-07	2.6928E-07
1-Propanol	0.46131	5.8180E-08	8.7270E-08	1.1636E-07	1.4545E-07	1.7454E-07	2.0363E-07	2.3272E-07

Table 5. Results of CT rate production N3- ZnS devices system at $\Delta^0 = 0.27\ (eV)$ with $T = 300\ K$.

solvent	$\Lambda_{N3/ZnS}(eV)$	**Rate of Electronic Transfer cm^2/ Sec** $\langle \mathcal{H}_{\frac{N3}{ZnS}} \rangle$ **(eV)^2**						
		1×10^{-3}	**1.5×10^{-3}**	**2×10^{-3}**	**2.5×10^{-3}**	**3×10^{-3}**	**3.5×10^{-3}**	**4×10^{-3}**
Chloroform	0.24323	3.8182E-08	5.7273E-08	7.6363E-08	9.5454E-08	1.1455E-07	1.3364E-07	1.5273E-07
1,2-Dichloroethane	0.36421	2.5368E-08	3.8052E-08	5.0736E-08	6.3420E-08	7.6104E-08	8.8788E-08	1.0147E-07
1-Methyl-2-pyrrolidinone	0.43471	1.6079E-08	2.4118E-08	3.2158E-08	4.0197E-08	4.8237E-08	5.6276E-08	6.4316E-08
1-Butanol	0.44411	1.5033E-08	2.2550E-08	3.0067E-08	3.7583E-08	4.5100E-08	5.2617E-08	6.0133E-08
1-Propanol	0.46131	1.3253E-08	1.9880E-08	2.6506E-08	3.3133E-08	3.9759E-08	4.6386E-08	5.3012E-08

Table 6. Results of CT rate production for N3- ZnS devices system at $\Delta^0 = 0.32\ (eV)$ with $T = 300\ K$.

solvent	$\Lambda_{N3/ZnS}(eV)$	Rate of Electronic Transfer cm^2/ Sec $\langle \widehat{\mathcal{H}}_{\frac{N3}{ZnS}} \rangle\ (\mathbf{eV})^2$						
		$\mathbf{1} \times \mathbf{10^{-3}}$	$\mathbf{1.5} \times \mathbf{10^{-3}}$	$\mathbf{2} \times \mathbf{10^{-3}}$	$\mathbf{2.5} \times \mathbf{10^{-3}}$	$\mathbf{3} \times \mathbf{10^{-3}}$	$\mathbf{3.5} \times \mathbf{10^{-3}}$	$\mathbf{4} \times \mathbf{10^{-3}}$
Chloroform	0.24323	4.5011E-09	6.7517E-09	9.0022E-09	1.1253E-08	1.3503E-08	1.5754E-08	1.8004E-08
1,2-Dichloroethane	0.36421	4.4138E-09	6.6207E-09	8.8276E-09	1.1034E-08	1.3241E-08	1.5448E-08	1.7655E-08
1-Methyl-2-pyrrolidinone	0.43471	3.1761E-09	4.7642E-09	6.3523E-09	7.9403E-09	9.5284E-09	1.1116E-08	1.2705E-08
1-Butanol	0.44411	3.0111E-09	4.5166E-09	6.0222E-09	7.5277E-09	9.0333E-09	1.0539E-08	1.2044E-08
1-Propanol	0.46131	2.7188E-09	4.0782E-09	5.4376E-09	6.7970E-09	8.1564E-09	9.5158E-09	1.0875E-08

4. Discussion

From the results obtained in **Table (3)**, it was found that the values of the transition energy are affected by the dielectric constant and refractive index of both ZnS semiconductors and the solvents used in this system, and it was shown that when the refractive index decreases and the dielectric constant increases, the values of the transition energy increase. In **Table (3**), the calculated results show that the maximum value of the transition energy was for 1-propanol with a value of 0.46131, and the lowest value of the transition energy was for Chloroform with a value of 0.24323. In **Table (4),** at 300 K, the charge carrier concentration $N_s = 1.4 \times 10^{20} m^{-3}$ and effective driving force $\Delta^0 = 0.22\ (eV)$, the charge transfer rate of the solvent Chloroform had the highest values compared to the other solvents used in the system, where the value of charge transfer rates reached 1.0622E-06 at the coupling force 4×10^{-3})(. Compared to the solvents used in this system for the same coupling strength, the lowest charge transfer rate was 2.3272E-07 for 1-propanol, as expected, the charge transfer rate increased with increasing coupling strength and decreased with increasing transition energy. In **Table (5**), when increasing the amount of effective driving force to $\Delta^0 = 0.27\ (eV)$ and for the same temperature and concentration of charge carriers, it was found that the charge transfer rate for chloroform solvent at 4×10^{-3}) (coupling force was (1.5273E-07) was the highest value obtained compared to the other solvents used, and the lowest value was (5.3012E-08) for 1-propanol at the same coupling strength.

As shown in **Table (6**), the effective driving force was equal to $\Delta^0 = 0.32\ (eV)$ at the same temperature and charge carrier concentration, and the charge transfer rates reached the highest values in chloroform solvent with a value of 1. 8004E-08 at a coupling strength of 4×10^{-3}) (and the lowest value obtained was 1.0875E-08 at a coupling strength of 4×10^{-3}) (in 1-propanol.From the results shown in Tables 4, 5 and 6, it was found that the charge transfer rate decreased when the effective driving force was increased and the transition energy increased, which limited the charge transfer processes in the N3-ZnS system and the results showed that the N3-ZnS device had the best charge transfer rates at the effective driving force $\Delta^0 = 0.22\ (eV)$ and Chloroform solvent compared to the other solvents used in this system.

5. Conclusion

In conclusion, the high electronic transition rates were obtained when solvents with low transition energies were used, based on a donor-acceptor model. The results indicated in force that the transition energy was affected by the dielectric constant and refractive index of both solvents and semiconductors. In heterogeneous N3-Zns devices, it was found that the electron flow rates increased as the transition energy of the system decreased and the effective driving force decreased, as the effective driving force affected the charge transfer rates; when it increased, the CT dynamics became more complex, leading to enhanced recombination rates and reduced efficiency of the excited electron injection from the dye to the semiconductor. The N3-ZnS system was favoured by the chloroform solvent with an effective driving force value of $\Delta^0 = 0.22\ (eV)$compared to the other solvents that were used.

Acknowledgment

The authors thank the Department of Physics, College of Education for Pure Science /Ibn Al-Haitham, University of Baghdad.

Conflict of Interest

Conflict of Interest. The authors declare that they have no conflicts of interest.

Funding

We hereby confirm that all the Figures and Tables in the manuscript are ours.

Ethical Clearance

The project was approved by the local ethical committee at the University of Baghdad

References

1. Cai B, Zhang Y, Feng J, Huang C, Ma T, Pan H. Highly efficient g-C3N4 supported ruthenium catalysts for the catalytic transfer hydrogenation of levulinic acid to liquid fuel γ-valerolactone. Renew Energy. 2021;177:652–662. https://doi.org/10.1016/j.renene.2021.05.159
2. He L, Guo Y, Kloo L. The dynamics of light-induced interfacial charge transfer of different dyes in dye-sensitized solar cells studied by ab initio molecular dynamics. Phys Chem Chem Phys. 2021;23(48):27171–27184. https://doi.org/10.1039/D1CP02412D
3. Mauri L, Colombo A, Dragonetti C, Roberto D, Fagnani F. Recent investigations on thiocyanate-free ruthenium(II) 2,2′-bipyridyl complexes for dye-sensitized solar cells. Molecules. 2021;26(24):7638. https://doi.org/10.3390/molecules26247638
4. Al Maadhede TS, Jumali MH, Al-Agealy HJ, Yap CC, Al-Douri Y. Improved performance of D149 dye-sensitized ZnO-based solar cell under solvents activation effect. Eur Phys J Plus. 2023;138(4):325. https://doi.org/10.1140/epjp/s13360-023-03935-0
5. Nahi N, Al-Agealy HJ, Moghaddam HM. Determining of efficiency for the N749 dye contact with TiO2 in dye-sensitized solar cell. Ibn Al-Haitham J Pure Appl Sci. 2024;37(1):187–197. https://doi.org/10.30526/37.1.3235
6. Al-Agealy HJ, Al-Hasan HH, Muslim RA, Hassooni MA. Theoretical calculation of the electronic current density in ruthenium 620 contact with TiO2 semiconductor in propanol solvent. J Theor Appl Phys. 2024;18. https://doi.org/10.57647/j.jtap.2024.si-AICIS23.18
7. Al-Agealy HJ, Hassooni MA, Ahmad MS, Noori RI, Jheil SS. A theoretical study of charge transport at Au/ZnSe and Au/ZnS interfaces devices. Ibn Al-Haitham J Pure Appl Sci. 2014;27(1):176–187.

8. Al-Agealy HJM, Al Maadhede TS, Jumali MH, Yap CC. A theoretical study of the influence of donor sensitizer dye on performance of dye-sensitized solar cells DSSCs. Ibn Al-Haitham J Pure Appl Sci. 2023;36(4):171–181. https://doi.org/10.30526/36.4.3382
9. Farah YR, Krummel AT. The N3/TiO2 interfacial structure is dependent on the pH conditions during sensitization. J Chem Phys. 2022;157(4). https://doi.org/10.1063/5.0099543
10. De Angelis F, Fantacci S, Selloni A. Alignment of the dye's molecular levels with the TiO2 band edges in dye-sensitized solar cells: a DFT–TDDFT study. Nanotechnology. 2008;19(42):424002. https://doi.org/10.1088/0957-4484/19/42/424002
11. Azpiroz JM, De Angelis F. DFT/TDDFT study of the adsorption of N3 and N719 dyes on ZnO ($10\bar{1}0$) surfaces. J Phys Chem A. 2014;118(31):5885–5893. https://doi.org/10.1021/jp501058x
12. Asaduzzaman AM, Schreckenbach G. Interactions of the N3 dye with the iodide redox shuttle: quantum chemical mechanistic studies of the dye regeneration in the dye-sensitized solar cell. Phys Chem Chem Phys. 2011;13:15148–15157. https://doi.org/10.1039/C1CP21168D
13. Ahmed Z, Rahman T, Hussain KM, Khatun MT, Chowdhury MS, Faruqe T, et al. Characterization and optimization of ZnS thin film properties synthesis via chemical bath deposition method for solar cell buffer layer. Main Group Chem. 2023;22(1):79–91. https://dx.doi.org/10.3233/mgc-210127
14. Mishra S, Haranath D. Synthesis, properties, and applications of zinc sulfide for solar cells. In: Nanoscale Compound Semiconductors and their Optoelectronics Applications. Woodhead Publ. 2022:47–66. https://doi.org/10.1016/B978-0-12-824062-5.00007-5
15. Ghadhban RQ, Al-Agealy HJ, Hassooni MA. Theoretical analysis of the electronic current at Au/PTCDA interface. NeuroQuantology. 2020;18(9):81.
16. Le Bellac M. *Quantum physics*. Cambridge University Press; 2011.
17. Levi AFJ. *Applied quantum mechanics*. Cambridge University Press; 2023.
18. Zettili N. *Quantum mechanics: concepts and applications*. Wiley; 2009.
19. Al-Agealy HJ, Hassooni MA. A theoretical study of the effect of the solvent type on the reorganization energies of dye-semiconductor system interface. Ibn Al-Haitham J Pure Appl Sci. 2017;23(3):51–57.
20. Ferry D. *Quantum mechanics: an introduction for device physicists and electrical engineers*. CRC Press; 2020. https://doi.org/10.1201/9781003031949
21. Berezhnoy YA. *The quantum world of nuclear physics*. Vol. 1. World Scientific; 2005.
22. Bushev M. *Synergetics: Chaos, order, self-organization*. World Scientific; 1994.
23. Vasko FT, Raichev OE. *Quantum kinetic theory and applications: Electrons, photons, phonons*. Springer; 2006.
24. Al-Agealy HJM, Hassoni MAH, Ahmad MS, Noori RI, Jheil SS. A theoretical study of charge transport at Au/ZnSe and Au/ZnS interfaces devices. Ibn Al-Haitham J Pure Appl Sci. 2013;27(1):176–187.
25. Hamann TW, Gstrein F, Brunschwig BS, Lewis NS. Measurement of the free-energy dependence of interfacial charge-transfer rate constants using ZnO/H2O semiconductor/liquid contacts. J Am Chem Soc. 2005;127(21):7815–7824.
26. Al-Agealy HJM, Hassooni MA. Calculate of the rate constant of electron transfer in TiO2–Safranine dye system. Ibn Al-Haitham J Pure Appl Sci. 2011;24(3).
27. Nazeeruddin MK, Kay A, Rodicio I, Humphry-Baker R, Müller E, Liska P, et al. Conversion of light to electricity by cis-X2bis(2,2′-bipyridyl-4,4′-dicarboxylate) ruthenium(II) charge-transfer sensitizers (X = Cl−, Br−, I−, CN−, SCN−) on nanocrystalline titanium dioxide electrodes. J Am Chem Soc. 1993;115(14):6382–6390. https://doi.org/10.1021/ja00067a063
28. Okutan M, Yakuphanoğlu F, Okutan MI, Bablich A, Haring Bolívar P. Dye-sensitized solar cell: Effect of light on N3 dye/BMII electrolyte based architecture. Phys B Condens Matter. 2024;685:416027. https://doi.org/10.1016/j.physb.2024.416027
29. Fleming JW, Weber MJ, Day GW, Feldman A, Chai BH, Kuzyk MG, et al. *Handbook of optical materials*. CRC Press; 2018. https://doi.org/10.1201/9781315219615

30. Patnaik P. *Handbook of inorganic chemicals*. Vol. 529. McGraw-Hill; 2003.
31. Smallwood I. *Handbook of organic solvent properties*. Butterworth-Heinemann; 2012.
32. Shah SS, Awan SU, Zainab S, Tariq H, Riaz MB, Ul-Haq A, et al. Decreasing of optical bandgap and N/P-type charge carriers variations in Cu doped ZnS thin films for buffer layer applications in solar cell devices. SSRN. 2023. https://doi.org/10.2139/ssrn.4349336
33. Lewis NS. Progress in understanding electron-transfer reactions at semiconductor/liquid interfaces. J Phys Chem B. 1998;102(25):4843–4855.
34. Hlynchuk S, Lancaster M, MacInnes M, Vasquez R, Maldonado S. Fundamental principles of semiconductor/electrolyte junctions. In: *Springer Handbook of Inorganic Photochemistry*. Springer; 2022:767–804. https://doi.org/10.1007/978-3-030-63713-2_27